Journal of Transactions in Systems Engineering
https://ijitis.org/index.php/JTSE
ISSN: 2806-2973
Volume 1, Issue 1
DOI: https://doi.org/10.15157/JTSE.2023.1.1.31-49
Received: 02.02.2023; Accepted: 11.03.2023

Environment Effect on Underwater Wet Welding Process of API 5L X65 Steel by Coating Resin-Based E6013 Electrode

Chandra Wijaya Hikmatullah*[1], Ipick Setiawan[1], Agus Pramono[2]

[1]Department of Mechanical Engineering, Sultan Ageng Tirtayasa University, 42435 Banten, Indonesia
[2]Department of Metallurgy Engineering, Sultan Ageng Tirtayasa University, 42435 Banten, Indonesia
***chandrahik25@gmail.com**

Abstract

The microstructure formed on the surface of API 5L X65 steel conducted underwater water wet welding is influenced by the surrounding environment and the selection of electrodes used. E6013 electrode coated with polyester resin was chosen to prove whether conventional electrodes can be used for underwater wet welding and minimize the price paid due to expensive special underwater welding electrodes. Optical microscopy and SEM-EDX tests were conducted to observe and analyse the phases formed on the surface of the specimens and to determine the chemical elements contained. Carbon deficiency occurs during the underwater wet welding process due to compound reactions. In this research work it has been seen that austenite and ferrite are the dominant phases due to the loss of carbon which affects the phases formed.

Keywords: *API 5L X65 steel, Microstructure, Shielded metal arc welding, Underwater wet welding*

INTRODUCTION

The development of technology and science results in many engineering applications. There are many types of construction on land and water. Underwater structures in offshore buildings are widely used to support the exploration and exploitation of mining materials such as natural gas and petroleum. Regarding exploiting mining materials in the ocean like subsea drilling pipes are generally created from high-strength steel using American Petroleum Institute (API) rules. One type of steel used in subsea lines with API specifications is API 5L X65 steel [1]. API 5L X65 steel is widely used to deliver energy and transport oil and gas. API 5L X65 steel belongs to the high-resistance steel category [2].

Construction of underwater structures, such as subsea pipelines, when damaged, must be repaired immediately. Underwater welding is necessary because it can be used during emergencies and costs less than construction structures that must be brought ashore first. Underwater dry welding and underwater wet welding are types of underwater welding [3]. Underwater wet welding is done in water like welding on land where no barrier separates the arc from the water. This is a simple method that can be used in welding. The potential for steel welds in wet environments cannot be separated from the potential for cold cracking. The cooling rate of land welding is two to three times less than that of underwater wet welding, increasing the material's toughness but creating porosity. The consequences of the rapid cooling process have the effect of increasing the hardness value and decreasing the impact value in the heat affected zone (HAZ) due to the cooling structure formed the weld metal has porosity where the slag is trapped and the appearance of the weld is not as neat as welding on land. This phenomenon affects water depth, electrode coating, hydrogen diffusion in the weld metal and arc stability. The disadvantages of underwater wet welds are the removal of alloy chemical compounds, increased carbon and oxygen content due to trapping in the weld, and increased tendency to crack. In addition, a chemical reaction occurs during welding,

where the alloy's chemical compounds react with hydrogen and oxygen from the split water molecules, changing the mechanical properties of the weld metal. Manganese and carbon composition variations affect hardenability, while oxygen content variations can affect toughness. Hydrogen diffusion and associated cracks are significant problems in underwater welding. The energy from the electric arc dissociates water into hydrogen and oxygen in the molecular [4].

The welded outer frame (watertight chamber) covered with a gas mixture at room pressure is an underwater dry welding process. While underwater wet welding is more desirable than underwater dry welding because it can cut costs and has high welder flexibility so that little places can be reached because it does not require a watertight chamber [3].

Underwater welding with the SMAW method can use special underwater welding or conventional coated electrodes. The electric current used to obtain the arc flame is similar to that used in land-based welding. In practice, wet welding is used underwater, directly exposed to a wet environment. Specialized or conventional coated electrodes may be used, and welding is done manually, as in land-based welding [4].

Underwater wet welding process conditions produce specimens with unique microstructures, such as electrode type, coating material, current strength, type of water used, and welding depth. In underwater wet welding, water can dissociate due to the influence of direct current during welding. In underwater wet welding, water molecules dissociate in the form of oxygen and hydrogen atoms in the arc plasma. The dissociated chemical elements (O- and H+) are dissolved in the molten metal through a mass transfer mechanism from the electrode tip to the weld material. This can oxidize the alloying elements and consequently modify the microstructure of the weld zone [5].

Our research will focus on the results of API 5L X65 steel welds performed underwater wet welding with the SMAW method. E6013 electrode coated with polyester resin coating is selected in this study, using welding currents of 60A, 90A, and 120A. In addition, optical microscopy and SEM-EDX tests were conducted. Serves to get the desired analysis, namely the phase formed in the weld area with each use of current, and analyse why the phase is developed based on the chemical compounds contained in the weld area and see the enlarged fracture using SEM.

MATERIALS & EXPERIMENT METHODS

API 5L X65 Steel

Various design solutions depend on many factors in mining and extracting crude oil and natural gas resources on the seabed. Such operations require such things as drilling into underground reservoirs and transporting goods. This can be done due to the high mechanical properties of the pipe material. In the case of deep water mining, rig casing and underwater transport pipes are usually made of high-strength steel per American Petroleum Institute (API) rules and ISO standards [1].

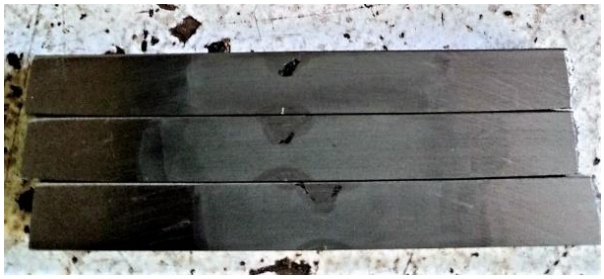

Figure 1. API 5L X65 steel

API 5L X65 steel is classified as low alloy steel with high durability, good ductility and weldability, and a low carbon content of less than 0.30%. This steel is used in high-pressure pipeline construction, so this material is recommended to support high internal pressure [2].

Table 1 depict chemical composition of API 5L X65.

Table 1. API 5L X65 steel chemical composition

Chemical Composition (%)							
C	**Si**	**Mn**	**P**	**S**	**Al**	**Cr**	**B**
0,067	0,253	1,312	0,009	0,002	0,032	0,087	0,0003
Chemical Composition (%)							
Mo	**Ni**	**V**	**Cu**	**Nb**	**Ti**	**N**	
0,001	0,133	0,044	0,009	0,035	0,002	0,0029	

Underwater Welding

British Admiralty - Dockyard performed the first underwater welding to seal leaky ship rivets below the waterline. Underwater welding is an essential tool for underwater fabrication work. Several offshore structures, including oil rigs, pipes, and offshore platforms, have been installed in recent years due to their significant utility. These underwater structures may experience structural failure due to abnormal use or unexpected events such as storms. To repair these structures, underwater welding methods are required [6].

Underwater wet welding is performed in water, like welding on land, while there is no mechanical barrier between the arc and the water. They commonly used fusion welding techniques such as shielded metal arc welding, gas tungsten arc welding and metal inert gas welding for underwater welding. Shielded metal arc welding (SMAW) is one of the most straightforward processes that produce high-quality weld and high productivity with other advantages of low cost and welder flexibility. A type of stainless steel, carbon, and low alloy steel is located underwater when damage occurs, such as repairing and splicing processes using underwater welding. Steel welds in wet environments have a probability of cold cracking [4].

Underwater wet welding is known to increase porosity along the weld. There are several disadvantages in underwater wet welding, such as the presence of slag in the weld, the loss of alloying elements that can reduce the quality of the weld, and the increased carbon and oxygen content that of them can lead to cracking. The mechanical characteristics of the weld metal change because it chemically reacts between the alloying elements with carbon and the compounds found in water, namely hydrogen and oxygen. Manganese and carbon content variations affect hardenability, while oxygen content variations can affect toughness. Hydrogen diffusion and associated cracks are significant problems in underwater welding. The electric arc created during welding causes water to dissociate, and water will split into hydrogen and oxygen molecules [4].

Underwater dry welding requires a watertight chamber for the welding process so that the welder and the material being welded are not directly exposed to the wet environment. An impermeable chamber is installed along the construction structure where damage has occurred, and the chamber is filled with gas. Weld products made with this welding technique are more precise than underwater wet welding [3].

Although technological developments help to create an underwater chamber in the underwater wet welding method, it is constrained by high costs and specialized equipment. Dry rooms are commonly used for underwater repairs and fabrication. Welding without a dry chamber (underwater wet welding) is more desirable [4].

Electrode

Most SMAW welding electrodes are coated with a layer of flux. When the welding process is carried out, the gas formed from the flux can protect the metal from contamination by the surrounding air. Flux used in electrodes is several chemical elements mixed with welding needs. According to AWS (American Welding Society) standards, electrodes can be classified with the letter E and followed by four or five digits. They were marking electrodes with the code EXXXX. The letter E is the code for SMAW-wrapped electrodes, XX after E is the tensile strength that can be produced, then the third X is the welding position, and the last X is the type of flux used. Based on AWS, the E6013 electrode has a flux material made of high potassium titania; this material is low hydrogen and has a relatively low hydrogen content [7].

Coating

In underwater welding using the shielded metal arc welding (SMAW) technique, the type of current used is direct and mostly straight polarity, and the electrode must be watertight. With flux coated, it will cause bubbles during welding and transfer water from the welding arc to the weld pool area [6]. The coating on an electrode adheres to protect the substrate by imparting dimensional and surface properties to its base metal [8]. This coating process aims to protect the flux so that it is not directly wet exposed to a humid/wet environment, namely underwater. The coating function is so that the short only occurs at the tip of the electrode, and the current does not come out of the flux side of the electrode during the underwater wet welding process. A coating process is required to facilitate the arc at the end of the electrode.

Weld Area

There are several regions in the weld, which are the weld metal, heat affected zone and base metal. Base metal is part of the base metal where welding heat and temperature do not cause changes in structure and properties. The HAZ is the metal between the base metal and the weld metal. This area undergoes a thermal cycle of rapid heating and cooling during the welding process. The parent metal structure will gradually change to the weld metal structure in the HAZ region. The weld metal region is part of the metal where welding occurs, where the metal melts and solidifies afterward. Weld metal is produced from several materials derived from filler and base metal or flux because flux usually consists of certain ingredients in specific proportions [9].

RESULTS AND DISCUSSION

Microstructure Observation

The microstructure was observed using optical microscopy with a magnification of 100x, which had previously been etched with nital. The areas observed and analysed are the base metal, HAZ and weld metal with each variable current when welding is 60A, 90A and 120A, see Figures 2 until 4. It has been seen the microstructure of the base metal of API 5L X65 steel. The microstructure of the base metal is a combined alloy of austenite, ferrite, and pearlite. Austenite decreases hardness. At the same time, pearlite is austenite that transforms into two mixed phases: ferrite and cementite. In the base metal area, it can be seen that the most dominating ferrite area.

Furthermore, the microstructure of the HAZ region at currents of 60A, 90A, and 120A can be observed in Figures 5 until 7.

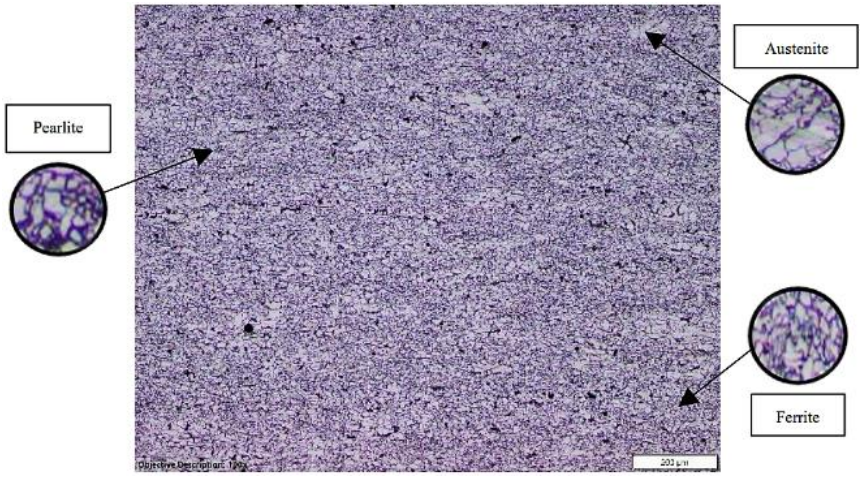

Figure 2. Microstructure of base metal current 60A magnification 100x

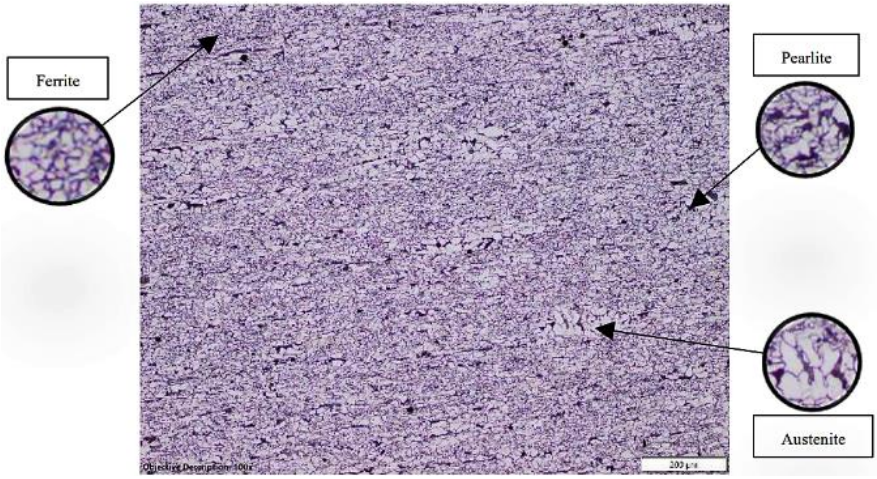

Figure 3. Microstructure of base metal current 90A magnification 100x

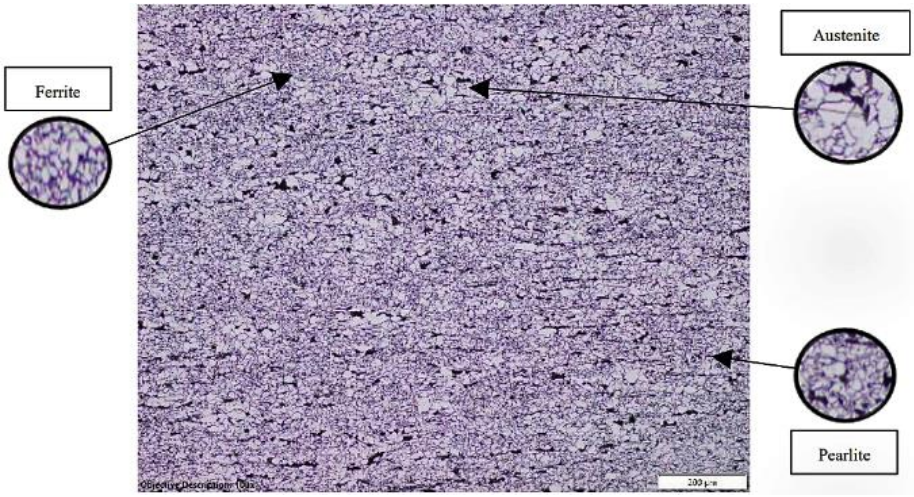

Figure 4. Microstructure of base metal current 120A magnification 100x

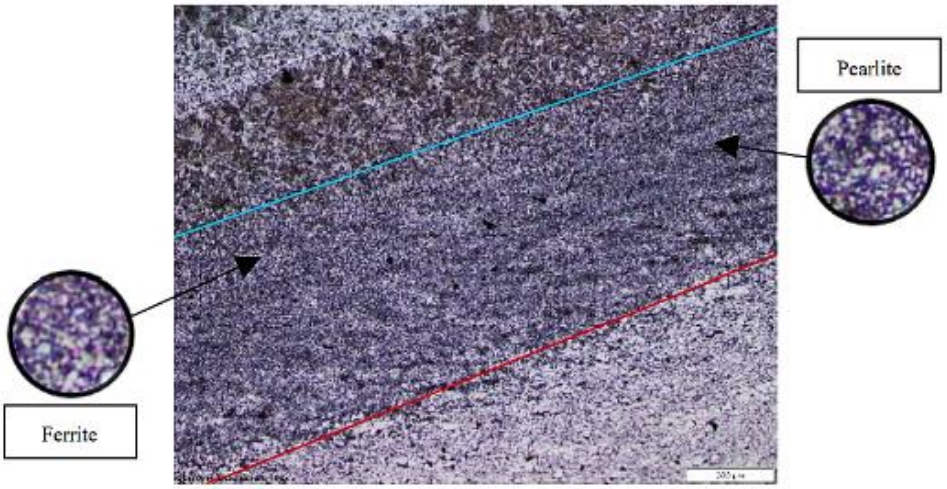

Figure 5. Microstructure of HAZ current 60A magnification 100x

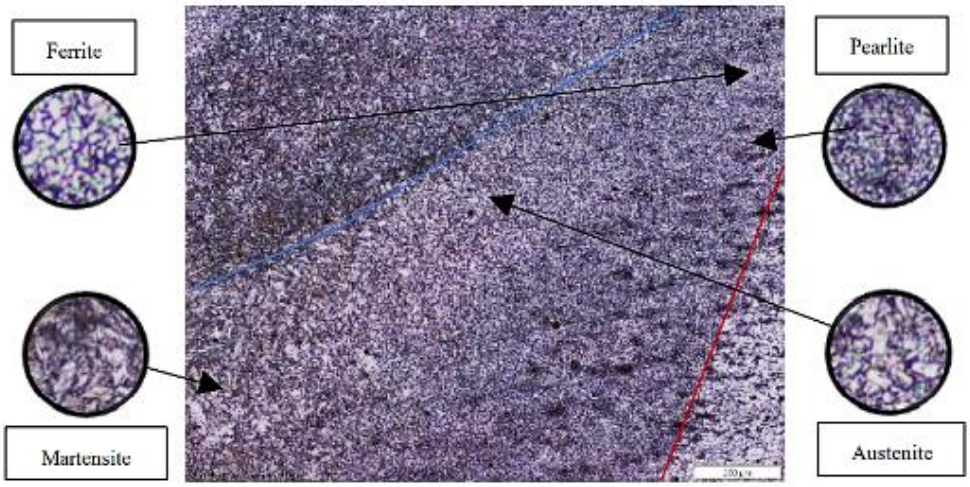

Figure 6. Microstructure of HAZ current 90A magnification 100x

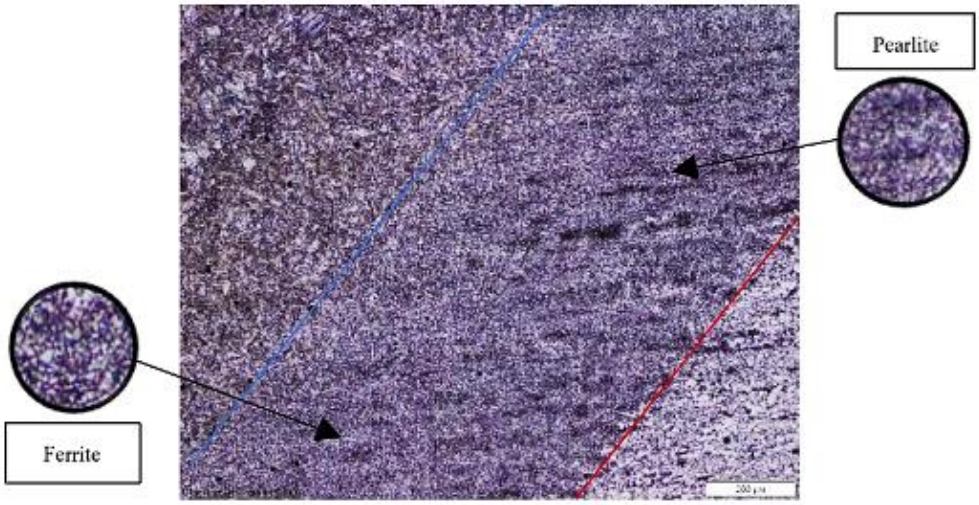

Figure 7. Microstructure of HAZ current 120A magnification 100x

In the Figure 5 until 7 it has been seen that the higher of the welding current used, the wider the HAZ area. This can be seen from the striking boundaries between the base metal, HAZ, and weld metal areas. The blue line is the boundary between the weld metal and HAZ, and the red line is the boundary between HAZ and base metal.

At a current of 90A, there are FGHAZ and CGHAZ areas, where for the FGHAZ area, there is a lot of pearlite and ferrite, while in the CGHAZ area, there is martensite and austenite. For currents of 60A and 120A, there is only pearlite and ferrite.

Figures 8, 9 and 10 depicts the microstructures of the weld metal current at 60A, 90A and 120A.

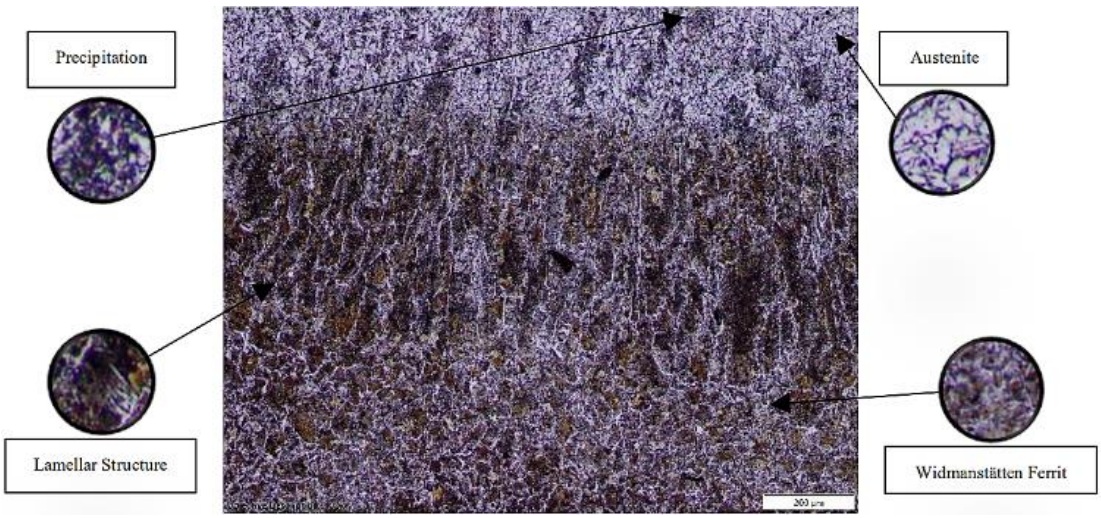

Figure 8. Microstructure of weld metal current 60A magnification 100x

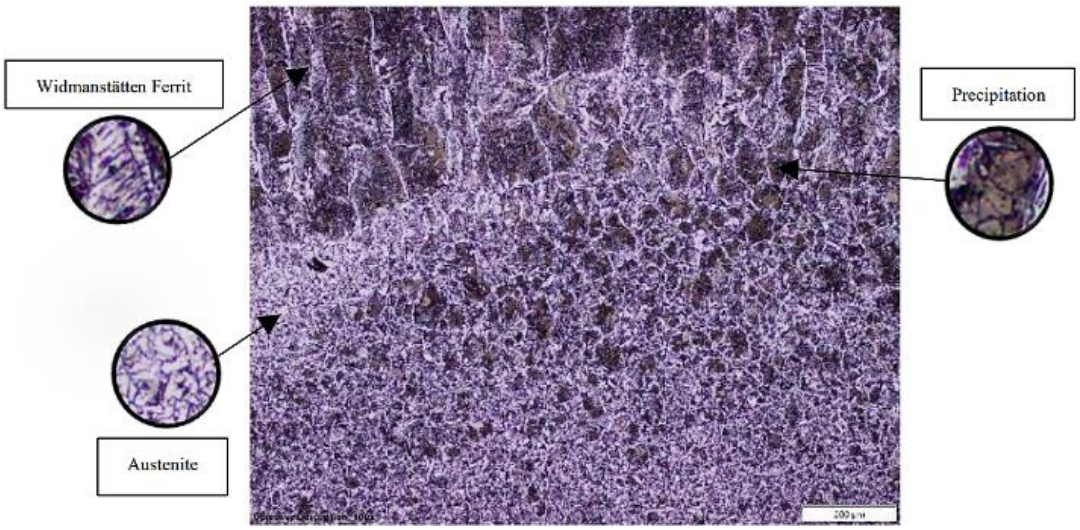

Figure 9. Microstructure of weld metal current 90A magnification 100x

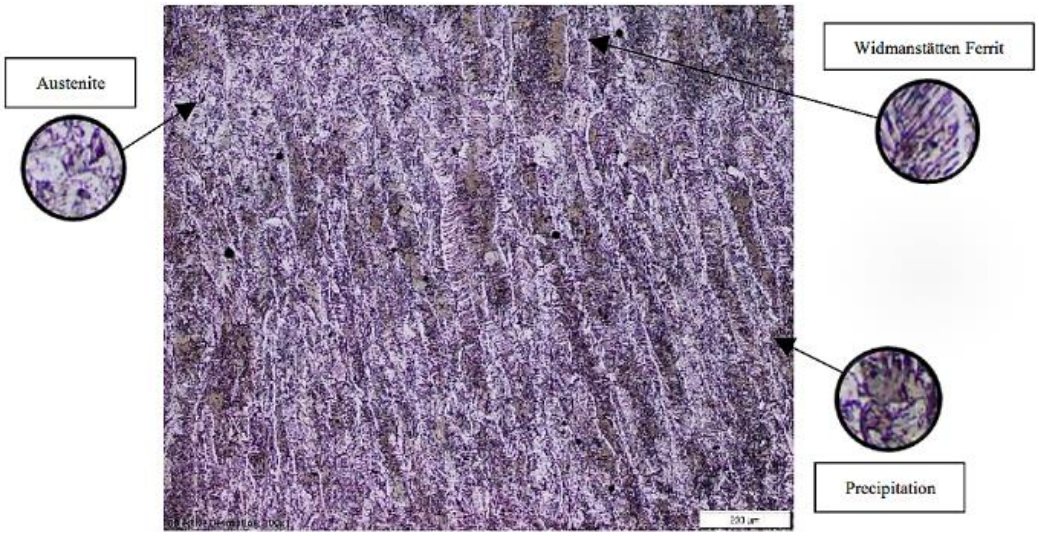

Figure 10. Microstructure of weld metal current 120A magnification 100x

E6013 electrode produces the most minor and lowest size porosity with the most stable arc. Therefore, the E6013 electrode is recommended for underwater wet welding. At 60A current, there are many lamellar structure regions. The effect of the heat treatment dissolves the carbides derived from the alloy, and the insoluble carbon precipitates as lamellae upon the cooling process. Due to the quenching effect, which is the rapid cooling of the metal from the heat during underwater wet welding, the metal phase has yet to form ideally.

At all currents used, there is precipitation on the surface. Separating a new phase from a solid or liquid phase is usually due to a change in temperature, pressure, or both. Underwater wet welding certainly affects temperature changes because it produces a quenching effect on the specimen. This transformation generally results in a mixture of phases from the initial saturated phase. The resulting phase has a crystal structure similar to the parent phase but has a different chemical composition and temperature parameters. Alloy phases have different microstructural sizes and shapes, so the physical, chemical and mechanical properties are also other.

Widmanstätten is a structure characterized by geometric patterns resulting from forming new phases along certain crystallographic planes of the solid parent solution. At high enough temperatures during the homogenization process, the specimens produce microstructures that obscure the shape of the original structure, such as the widmanstätten ferrite phase found in the microstructure test results.

Metallography and Chemical Composition Analysis

The Scanning Electron Microscopy-Energy Dispersive X-ray (SEM-EDX) method was used to study the microstructure. SEM serves to investigate the fracture surface. EDX analysis was also performed to investigate the chemical composition. The surface of API 5L X65 steel specimens subjected to underwater wet welding was analyzed using SEM. Figures 11, 12 and 13 depict the fractures of API 5L X65 steel specimens subjected to underwater wet welding with each current used.

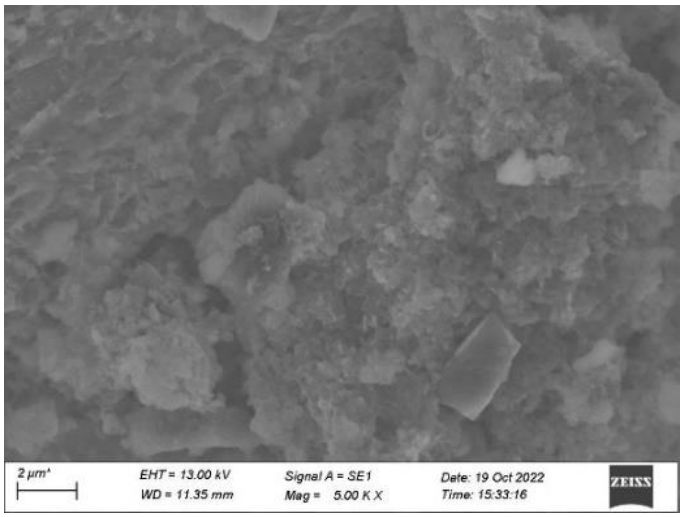

Figure 11. SEM image of the fracture using 60A current

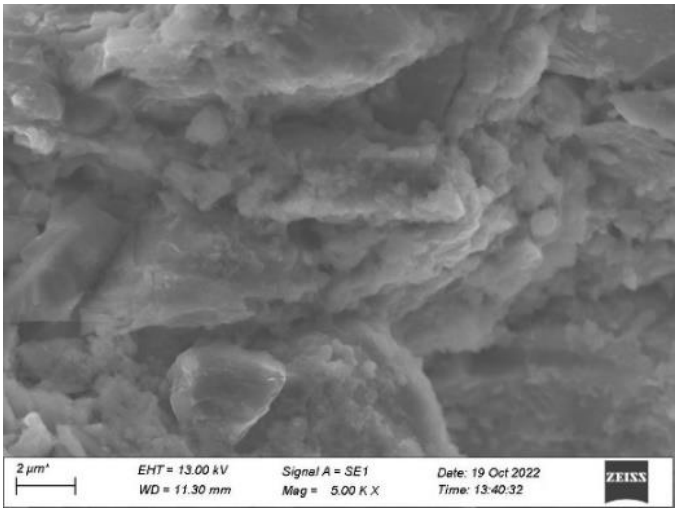

Figure 12. SEM image of the fracture using 90A current

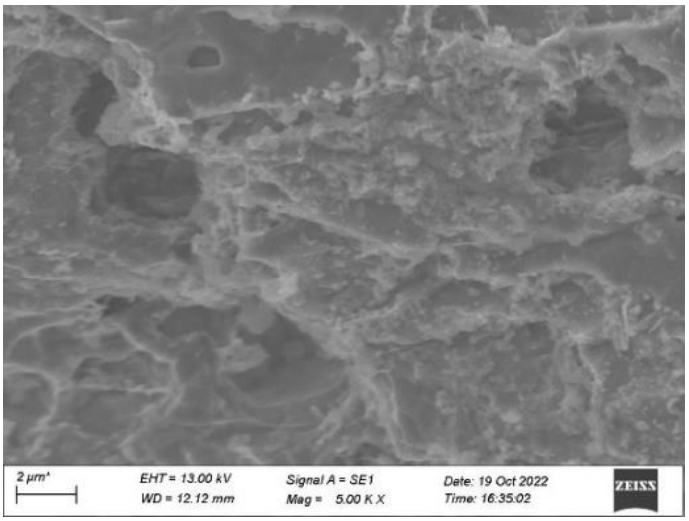

Figure 13. SEM image of the fracture using 120A current

Analysis of the fracture with SEM shows that the fracture surface area consists of micro-holes on the fracture surface of the 90A and 120A current specimens. In contrast, on the fracture surface of the 60A current specimen, the grain is still attached to the fracture surface. The greater the current user, the greater the area of dimples on the surface of the fracture. It can be seen in the fault area of the 120A current specimen more dimples area compared to the fault area of the 60A current specimen. Thus, it can be concluded that the specimen with a current of 120A in the weld area is more ductile than the weld area in the 60A specimen, which is confirmed by the scattered dimples area.

In the base metal area, heat affected zone, weld metal and fracture area, with each use of current, EDX analysis is carried out to see what elements are found in the area, see Figure 14.

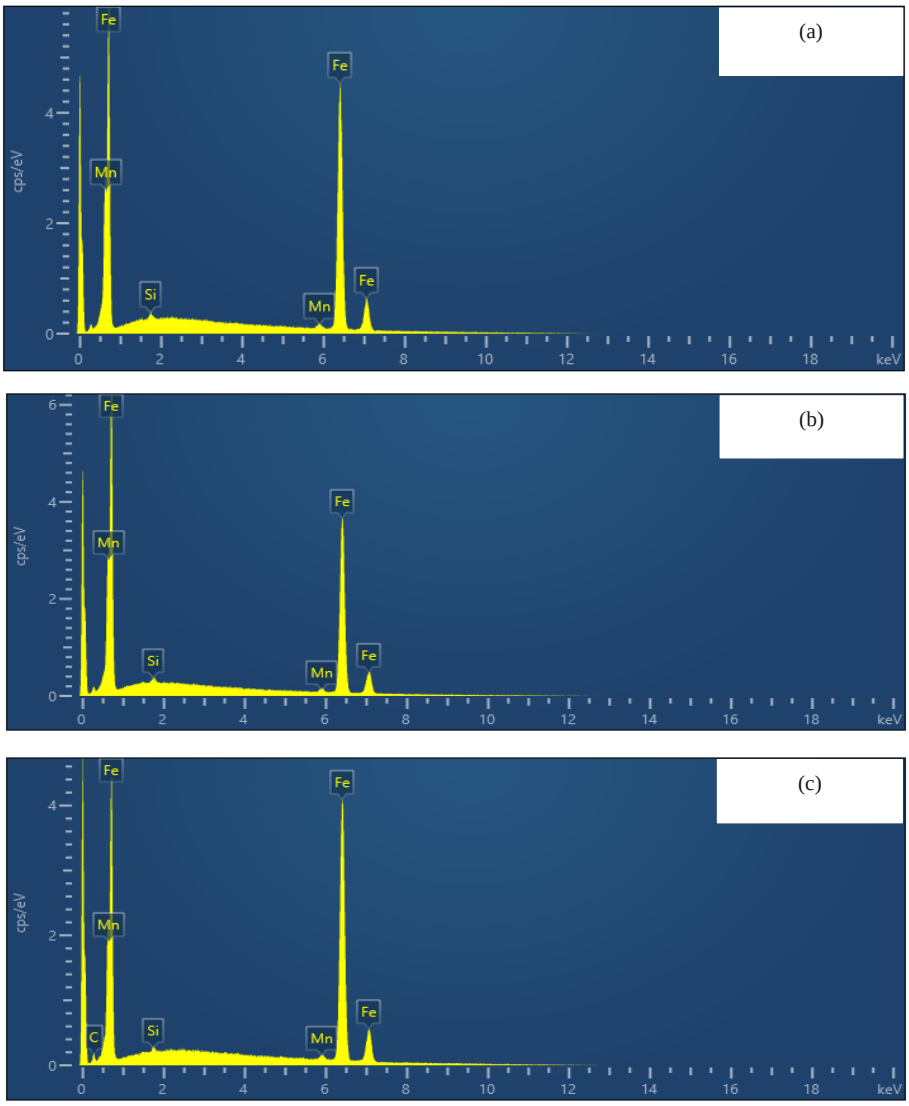

Figure 14. EDX analysis of base metal surface areas; (a) using 60A current, (b) using 90A current, (c) using 120A current

In the Tables 2 until 4 are shown the chemical composition on spectrum base metal 60A, 90A and 120A.

Table 2. Chemical composition on spectrum base metal 60A

Spectrum Base Metal 60A		
Element	**Weight %**	**Atomic %**
Si	0,27	0,54
Mn	1,68	1,70
Fe	98,05	97,75
Total	**100,00**	**100,00**

In the EDX test results for the 60A current base metal spectrum, it is known that the element iron (Fe) is the majority of elements found on the surface of the 60A current base metal, namely 98.05%. And found the element silicon (Si) at 0.27% and manganese (Mn) at 1.68%.

Table 3. Chemical composition on spectrum base metal 90A

Spectrum Base Metal 90A		
Element	**Weight %**	**Atomic %**
Si	0,26	0,51
Mn	1,43	1,45
Fe	98,31	98,04
Total	**100,00**	**100,00**

In the EDX test results for the 90A current base metal spectrum, it is known that the element iron (Fe) is the element most commonly found on the surface of the 90A current base metal, which is 98.31%. And the element silicon (Si) was seen at 0.26% and manganese (Mn) at 1.43%.

Table 4. Chemical composition on spectrum base metal 120A

Spectrum Base Metal 120A		
Element	**Weight %**	**Atomic %**
C	2,36	10,07
Si	0,21	0,39
Mn	1,20	1,12
Fe	96,23	88,42
Total	**100,00**	**100,00**

In the EDX test results for the 120A current base metal spectrum, it is known that the element iron (Fe) is the majority of elements found on the surface of the 120A current base metal, which is 96.23%. And found the element silicon (Si) at 0.21%, manganese (Mn) at 1.20%, and carbon (C) at 2.36%.

Figure 15 depict EDX analysis of HAZ surface areas by using 60A 90A and 120A current.

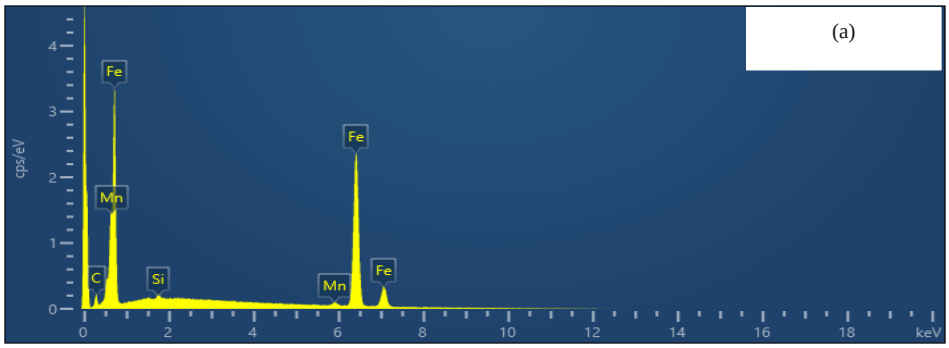

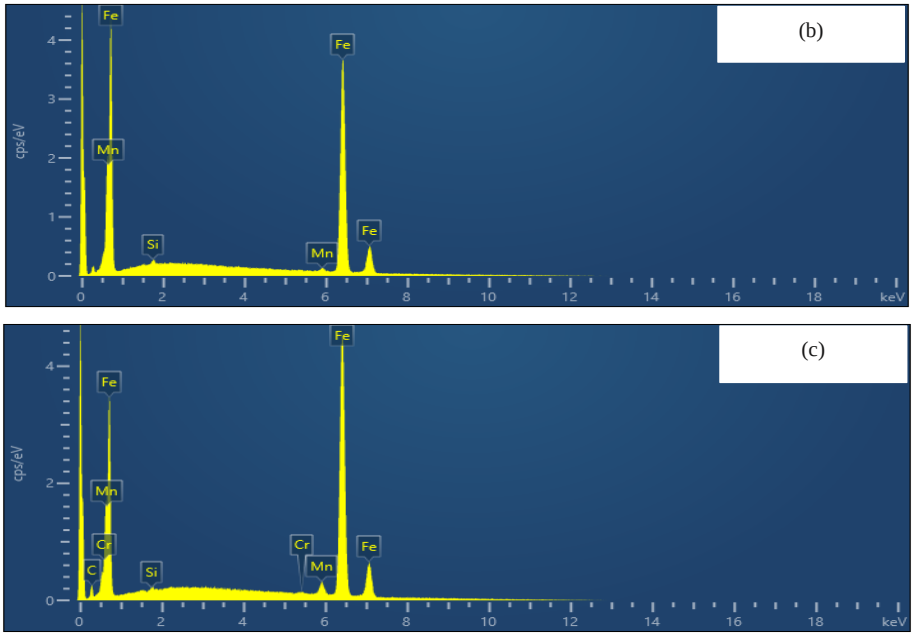

Figure 15. EDX analysis of HAZ surface areas; (a) using 60A current, (b) using 90A current, (c) using 120A current

In the Tables 5 until 7 are shown the chemical composition on spectrum HAZ 60A, 90A and 120A.

Table 5. Chemical composition on spectrum HAZ 60A

Spectrum HAZ 60A		
Element	**Weight %**	**Atomic %**
C	5,09	19,91
Si	0,25	0,43
Mn	1,42	1,21
Fe	93,24	78,46
Total	**100,00**	**100,00**

In the EDX test results for the 60A current HAZ spectrum, it is known that the element iron (Fe) is the element most commonly found on the surface of the 60A current HAZ, which is 93.24%. And found the element silicon (Si) by 0.25%, manganese (Mn) by 1.42%, and carbon (C) by 5.09%.

Table 6. Chemical composition on spectrum HAZ 90A

Spectrum HAZ 90A		
Element	**Weight %**	**Atomic %**
Si	0,23	0,45
Mn	1,05	1,07
Fe	98,72	98,48
Total	**100,00**	**100,00**

In the EDX test results for the 90A current HAZ spectrum, it is known that the element iron (Fe) is the majority of elements found on the surface of the 90A current HAZ, which is 98.34%. And found the element silicon (Si) by 0.27% and manganese (Mn) by 1.39%.

Table 7. Chemical composition on spectrum HAZ 120A

Spectrum HAZ 120A		
Element	**Weight %**	**Atomic %**
C	3,18	13,23
Si	0,12	0,22
Cr	0,25	0,24
Mn	3,16	2,87
Fe	93,29	83,44
Total	**100,00**	**100,00**

In the EDX test results for the HAZ spectrum of 120A current, it is known that the element iron (Fe) is the majority of elements contained in the HAZ surface of 120A current which correspond to 93.29%. As well as found elements of silicon (Si) by 0.12%, manganese (Mn) by 3.16%, chromium (Cr) by 0.25% and carbon (C) by 8.70%.

Figure 16 depict EDX analysis of weld metal surface areas by using 60A 90A and 120A current.

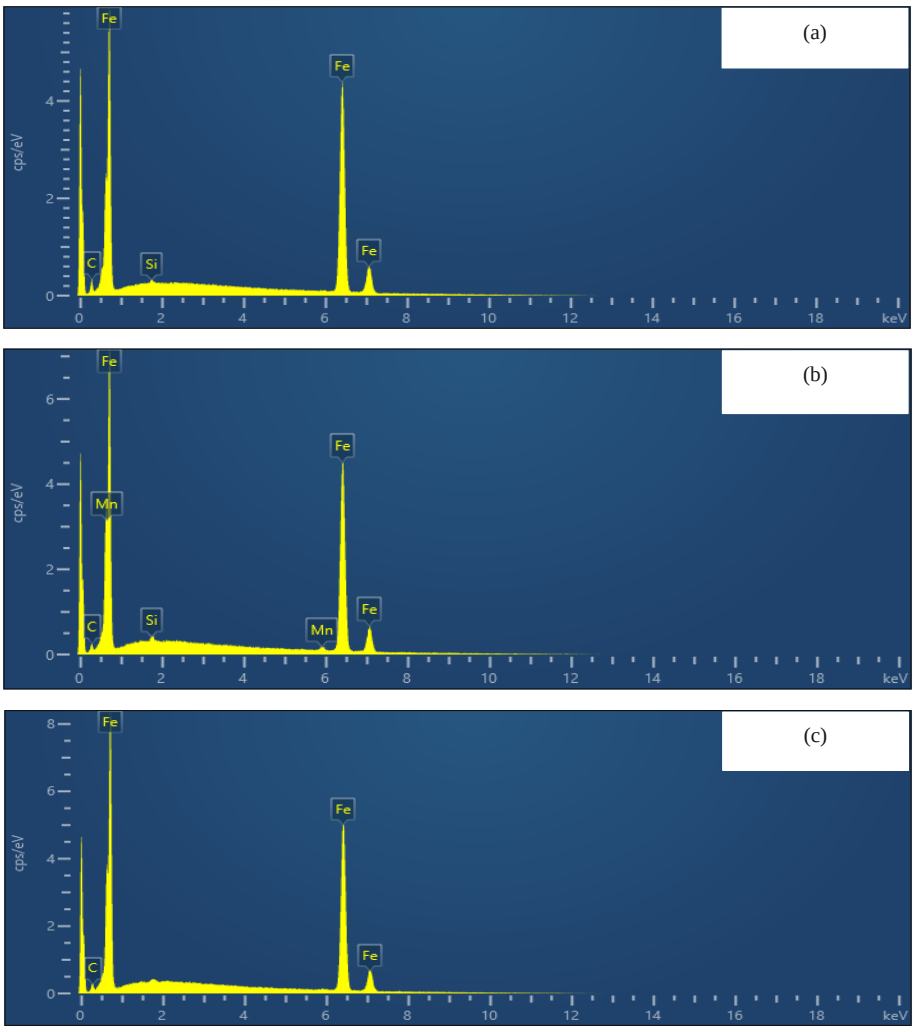

Figure 16. EDX analysis of weld metal surface areas; (a) using 60A current, (b) using 90A current, (c) using 120A current

In the Tables 8 until 10 are shown the chemical composition of the weld metal HAZ 60A, 90A and 120A.

Table 8. Chemical composition on spectrum weld metal 60A

Spectrum Weld Metal 60A		
Element	**Weight %**	**Atomic %**
C	4,15	16,75
Si	0,17	0,29
Fe	95,68	82,96
Total	**100,00**	**100,00**

In the EDX test results for the 60A current weld metal spectrum, it is known that the element iron (Fe) is the majority of elements found on the surface of the 60A current weld, namely 95.86%. And found the element silicon (Si) by 0.17% and carbon (C) by 4.15%.

Table 9. Chemical composition on spectrum weld metal 90A

Spectrum Weld Metal 90A		
Element	**Weight %**	**Atomic %**
C	2,69	11,36
Si	0,29	0,53
Mn	1,40	1,29
Fe	95,62	86,82
Total	**100,00**	**100,00**

In the EDX test results for the 90A current weld metal spectrum, it is known that the element iron (Fe) is the majority of elements contained on the surface of the 90A current weld, namely 95.62%. As well as found the element silicon (Si) by 0.29%, manganese (Mn) by 1.40% and carbon (C) by 2.69%.

Table 10. Chemical composition on spectrum weld metal 120A

Spectrum Weld Metal 120A		
Element	**Weight %**	**Atomic %**
C	2,89	12,15
Fe	97,11	87,85
Total	**100,00**	**100,00**

In the EDX test results for the 120A current weld metal spectrum, it is known that the element iron (Fe) is the majority of elements found on the surface of the 120A current weld, namely 97.11%. And found the element carbon (C) of 2.89%.

Figure 17 depict EDX analysis of fracture area surface areas by using 60A 90A and 120A current.

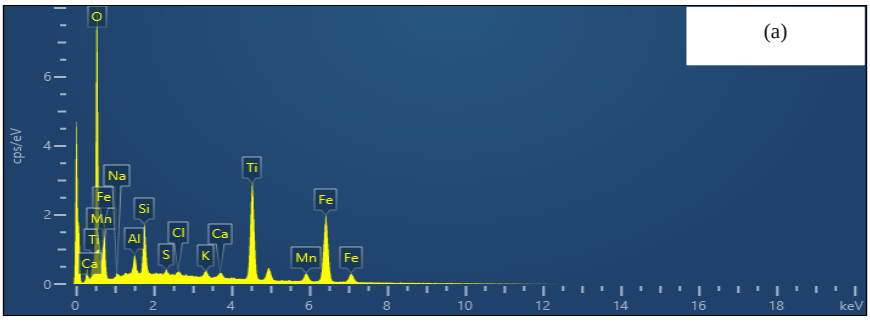

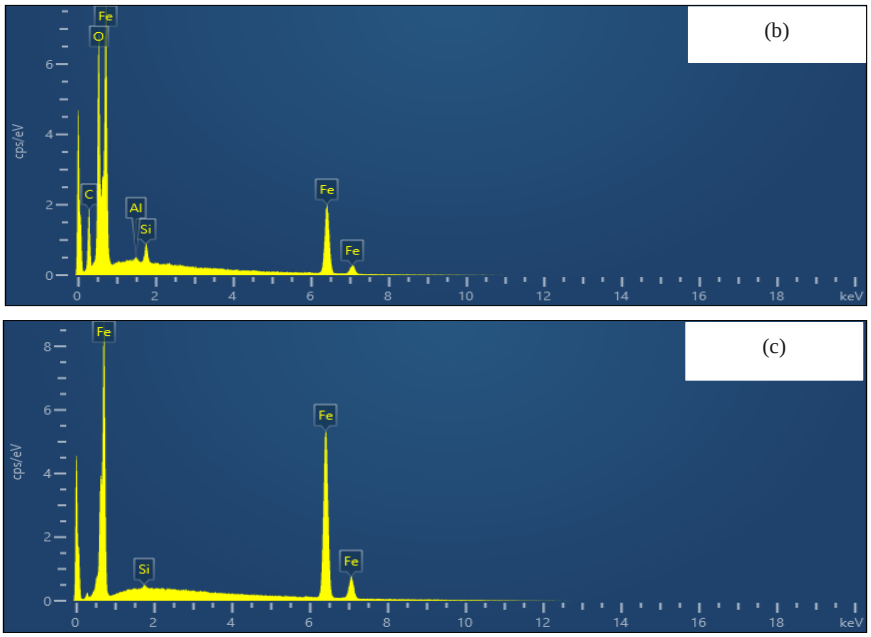

Figure 17. EDX analysis of fracture area surface areas; (a) using 60A current, (b) using 90A current, (c) using 120A current

In the EDX test results for the spectrum of the 60A current fracture area, it is known that the element iron (Fe) is the most elements found on the surface of the 60A current fault, namely 37.94%. As well as the details of oxygen (O) by 32.29%, sodium (Na) by 0.37%, aluminum (Al) by 1.09%, silicon (Si) by 2.86%, sulfur (S) by 0.32%, chlorine (Cl) by 0.29%, potassium (K) by 0.67%, calcium (Ca) by 0.63%, titanium (Ti) by 20% and manganese (Mn) by 3.54%. The following is a table of EDX results on the 60A current fault area.

In the Tables 11 until 13 are shown the chemical composition of the spectrum fracture area 60A, 90A and 120A.

Table 11. Chemical composition on spectrum fracture area 60A

Spectrum Fracture Area 60A		
Element	**Weight %**	**Atomic %**
O	32,29	59,55
Na	0,37	0,47
Al	1,09	1,19
Si	2,86	3,01
S	0,32	0,30
Cl	0,29	0,25
K	0,67	0,51
Ca	0,63	0,46
Ti	20,00	12,32
Mn	3,54	1,90
Fe	37,94	20,04
Total	**100,00**	**100,00**

Table 12. Chemical composition on spectrum fracture area 90A

Spectrum Fracture Area 90A		
Element	**Weight %**	**Atomic %**
C	20,89	40,48
O	24,89	36,21
Al	0,29	0,25
Si	1,40	1,16
Fe	52,54	21,90
Total	**100,00**	**100,00**

In the EDX test results for the fracture spectrum of the 90A current area, it is known that the element iron (Fe) is the most found on the surface of the 90A current fracture, which is 52.54%. As well as the element carbon (C) at 20.89%, oxygen (O) at 24.89%, aluminum (Al) at 0.29% and silicon (Si) at 1.40%.

Table 13. Chemical composition on spectrum fracture area 120A

Spectrum Fracture Area 120A		
Element	**Weight %**	**Atomic %**
Si	0,22	0,45
Fe	99,78	99,55
Total	**100,00**	**100,00**

In the EDX test results for the 120A current region, it is known that there are only two elements, namely iron (Fe) and silicon (Si), with wt% of 99.78% and 0.22%, respectively.

The eutectoid group includes manganese, iron, chromium, cobalt, nickel, copper and silicon. Two other elements often combined in titanium are tin and zirconium. These elements have solid solubilities in the α phase and the paratactically formed β phase of the metal. Although the elements do not favor phase stability, i.e., inhibit the transformation rate, they are helpful as strengthening agents. Elements such as aluminum and oxygen can increase the temperature at which the α phase stabilizes, useful as alpha (α) stabilizers. The silver brown pattern formed on the specimen indicates the presence of sulfur in the steel.

Water is a reactant dissociating into hydrogen and oxygen under direct current (DC) influence in water electrolysis. The chemical reaction equation follows [10].

$$H_2O \rightarrow H_2 + \frac{1}{2} O_2$$

The use of resin for coating is so that the flux core is not moist / exposed to water. Polyester resin has several advantages: good corrosion resistance, low weight, and low cost [11]. Polyester resin ($C_{10}H_8O_4$) burns at temperatures around 400-500 ^oC. When the resin is at a specific temperature and burns, oxidation occurs in which there will be a binding/coupling reaction by oxygen from electrolyzed water compounds to form other combinations. The chemical reaction equation follows.

$$C_{10}H_8O_4 + \frac{1}{2} O_2 \rightarrow 10\ CO_2 + 4\ H_2O$$

$$C_{10}H_8O_4 + 20(\frac{1}{2} O_2) \rightarrow 10\ CO_2 + 4\ H_2O$$

$$C_{10}H_8O_4 + 10\ O_2 \rightarrow 10\ CO_2 + 4\ H_2O$$

Due to the reaction process of the resin requires 20 times the O_2 from the electrolysis process, the coefficient of the H_2 compound becomes 20 as well. During the welding process, the hydrogen compound (H) in the remaining water electrolysis process will form a hydrocarbon compound (C_xH_y) with carbon (C). Where carbon (C) is one of the contents of API 5L X65 Steel material and E6013 electrode. The following is the chemical compound reaction equation.

$$20\ H_2 + 10\ C \rightarrow 10\ CH_4$$

The hydrocarbon reaction that occurs will form methane (CH_4) in the form of gas. Methane is the primary fuel source, and in the presence of oxygen (O_2), there will be a combustion reaction on methane. Here is the chemical reaction equation if methane reacts with oxygen.

$$10\ CH_4 + O_2 \rightarrow 10\ CO_2 + H_2O$$

$$10\ CH_4 + 20\ O_2 \rightarrow 10\ CO_2 + 20\ H_2O$$

Blow holes on the base metal's surface result from the effect of carbon loss (carbon deficiency) during the underwater wet welding process because it reacts with other elements.

The loss of Carbon (C) element is proven by optical microscopy testing and SEM-EDX. From the results of optical microscopy, it can be seen that the surface area of the weld, with the use of currents 60A, 90A, and 120A, formed austenite and ferrite phases. The carbon in the ferrite phase is ≤ 1%, and precipitation at all current strengths is used. Precipitation indicates a precipitate phase due to the quenching effect when welding. Then, there is a lamellar structure on the surface of the 60A current, which is carbon deposited as a lamella.

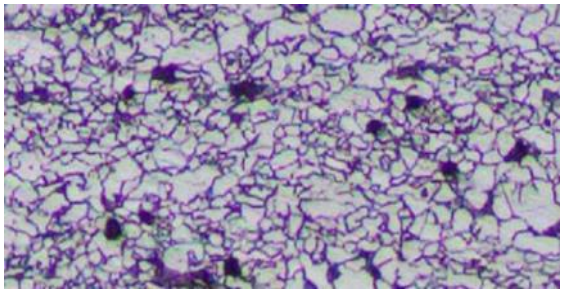

Figure 18. Base metal surface area

From SEM testing, it can be seen from the brittle fracture in terms of micro-holes and dimples formed. Very few dimples are included, even almost none using 60A current. As the current increases, more and more dimples are formed.

CONCLUSION

The increase in current strength used affects the microstructure formed. From the analysis of the microstructure of the weld metal area at a current of 60A, there is a lamellar structure, namely carbon deposition, on the surface of the specimen. When welding, the higher current can minimize the lamellar structure area formed. Austenite and ferrite are the dominating phases. This is due to the loss of carbon which affects the phases formed. The effect of rapid cooling during underwater wet welding creates a quenching effect on the surface microstructure, namely the creation of precipitation. The increase in current strength impacts the smaller lamellar structure area and the extent of the precipitation area. The chemical composition test results found that in some specimens, no carbon element was found. EDX tested the base metal, HAZ, weld metal and fracture areas with three times of data collection each for all current variables. From the total EDX test conducted, 36

data were obtained, with 20 data of which no carbon was found. Carbon deficiency occurs which correspond to the carbon loss during the underwater wet welding process due to compound reactions. Water molecules dissociate into oxygen and hydrogen elements, in which hydrogen reacts with carbon in the specimen to form hydrocarbon compounds. After the formation of hydrocarbon compounds and combustion, another compound is formed, namely carbon dioxide. Carbon loss is also due to strong currents during the underwater wet welding process, thus affecting the formation of phases.

ACKNOWLEDGMENT

The author would like to thank Mr. Darito and Mr. Samanhudi, Staff of PT Krakatau Pipe Industries, for providing API 5L X65 steel and the Welding Development Special Training Center, Condet, East Jakarta, for giving the underwater welding research site.

CONFLICT OF INTERESTS

The authors should confirm that there is no conflict of interests associated with this publication.

REFERENCES

[1] Rogalski G., Fydrych D. and Łabanowski J. Underwater Wet Repair Welding of API 5L X65M Pipeline Steel. *Polish Maritime Research*. 2017; 24(1); 188–194.

[2] De Oliveira M.C., Figueredo R.M., Acciari H.A. and Codaro E.N. Corrosion Behavior of API 5L X65 Steel Subject to Plastic Deformation. *Journal of Materials Research and Technology*. 2018; 7(3); 314–318.

[3] Barnabas S.G., Rajakarunakaran S., Pandian G.S., Buhari A.M.I. and Muralidharan V. Review on Enhancement Techniques Necessary for The Improvement of Underwater Welding. *Materials Today: Proceedings*. 2021; 45; 1191–1195.

[4] Vashishtha P., Wattal R., Pandey S. and Bhadauria N. Problems Encountered in Underwater Welding and Remedies- A Review. *Materials Today: Proceedings*. 2022; 64; 1433–1439.

[5] Ramírez Luna L.E., Bracarense A.Q., Pessoa E.C.P., Costa P.S., Altamirano Guerrero G. and Salas Reyes A.E. Effect of The Welding Angle on The Porosity of Underwater Wet Welds Performed in Overhead Position at Different Simulated Depths. *Journal of Materials Processing Technology*. 2021; 294; 117114.

[6] Sundarapandiyan C., Balamurugan A. and Mohan M. A Review on Under Water Welding Process. *International Journal of Innovations in Engineering and Technology*. 2017; 8(1); 260-265.

[7] Harahap J., Wahyudin W., Hasnita H. and Lutfhi L. Analisis Eksperimental dan Numerik Uji Tarik Hasil Pengelasan SMAW pada Baja Karbon Rendah dengan Variasi Jenis Elektroda Terhadap Sifat Mekanis. *VOCATECH: Vocational Education and Technology Journal*. 2022; 4(1); 8–17.

[8] Selly R., Rahmah S., Nasution H.I., Syahputra R.A. and Zubir M. Electroplating Method on Copper (Cu) Substrate with Silver (Ag) Coating Applied. *Indonesian Journal of Chemical Science and Technology*. 2020; 3(2); 38-41.

[9] Nurhasan M., Dirja I. and Setiawan R. Pengaruh Panas Terhadap Baja AISI 4340 pada Daerah HAZ, Logam Las, dan Bahan Induk Setelah Mengalami Pengelasan SMAW. *Jurnal Polimesin*. 2021;19(1); 81–87.

[10] Chi J., Yu H. Water Electrolysis Based on Renewable Energy for Hydrogen Production.

Chinese Journal of Catalysis. 2018; 39(3); 390–394.

[11] Barros M.M., de Oliveira M.F.L., da Conceição Ribeiro R.C., Bastos D.C. and de Oliveira M.G. Ecological Bricks from Dimension Stone Waste and Polyester Resin. *Construction and Building Materials*; 2020; 232; 117252.